Second order phase transitions from octupole-nondeformed to octupole-deformed shape in the alternating parity bands of nuclei around ^{240}Pu based on data

R. V. Jolos,[1,2,*] P. von Brentano,[2] and J. Jolie[2]
[1]*Joint Institute for Nuclear Research, 141980 Dubna, Russia*
[2]*Institut für Kernphysik der Universität zu Köln, 50937 Köln, Germany*
(Received 19 June 2012; published 30 August 2012)

Background: Shape phase transitions in finite quantal systems are very interesting phenomena of general physical interest. There is a very restricted number of the examples of nuclei demonstrating this phenomenon.
Purpose: Based on experimental excitation spectra, there is a second order phase transition in the alternating parity bands of some actinide nuclei.
Method: The mathematical techniques of supersymmetric quantum mechanics, two-center octupole wave functions ansatz, and the Landau theory of phase transitions are used to analyze the experimental data on alternating parity bands.
Results: The potential energy of the octupole collective motion is determined and analyzed for all observed values of the angular momentum of the alternating parity band states in ^{232}Th, ^{238}U, and ^{240}Pu.
Conclusion: It is shown that as a function of increasing angular momentum there is a second order phase transition from the octupole-nondeformed to the octupole-deformed shape in the considered nuclei.

DOI: 10.1103/PhysRevC.86.024319 PACS number(s): 21.10.Re, 21.10.Tg, 23.20.Lv, 27.70.+q

I. INTRODUCTION

Quantum phase transitions in an algebraic nuclear model, the interacting boson model (IBM), were studied in Refs. [1,2]. In recent years quantum phase transition phenomena in atomic nuclei came to the forefront of nuclear structure physics [3–11]. Mainly, the phase transitions among spherical, axially deformed, and γ-soft limits of nuclear structure have been analyzed. Of course, shape-transitional nuclei always attracted attention, but it was a difficult task to treat them. A possibility to analyze phase transition phenomena in nuclei in detail came with the formulation of the IBM. Its application has shown that, depending on the values of the control parameters, first and second order phase transitions occur. A consideration of the phase transition phenomena is closely related to the introduction by Iachello of the critical point symmetries in the collective Bohr-Mottelson model [12,13], which gave us simplified models for nuclei at the critical point. The model to describe the octupole motion at the critical point has been considered in Refs. [14–16].

In most considered cases the focus was on the quadrupole deformation and the role of the control parameters (i.e., the parameters of the IBM Hamiltonian), which are functions of the numbers of protons and neutrons in the nucleus. In the present paper we present and analyze an example of the second order phase transition in nuclei related to the octupole deformation, and the control parameter is the angular momentum. This is different from the study in Ref. [17] of the same shape phase transition as a function of neutron number but similar to one described in Ref. [18] for the quadrupole deformation. We mention that the situation described in this paper is different from the so-called excited state quantum phase transition [19,20]. We consider below a phase transition in the alternating parity bands from the reflection-symmetric to the reflection-asymmetric shape, or in other words, from octupole-nondeformed to octupole-deformed shape [21]. It was already indicated qualitatively [22–27] that the octupole deformation seems to stabilize with increasing angular momentum.

A confirmation of the existence of the second order phase transition in nuclei is very important and of general interest. The second order phase transition in the quadrupole shape of nuclei is closely related to the realization of the $E(5)$ critical-point symmetry [28,29]. The properties of many even-even nuclei have been examined in order to find examples displaying the characteristics of the $E(5)$ critical-point symmetry of the shape transition from the spherical vibrator to the triaxial soft rotor. Several examples of nuclei have been suggested [28,29] as candidates with the properties close to those predicted by the $E(5)$ symmetry.

It is the aim of the present paper to show, based on the experimental data, that an evolution of the reflection asymmetry in the alternating parity bands with increasing angular momentum gives a very clear example of a second order phase transition in nuclei.

In the consideration below we use a model which describes the collective octupole excitations of nuclei based on the assumption that the most important degree of freedom is β_{30}, which keeps axial symmetry. We thus assume a softness of the β_{30} mode, in contrast to the other octupole modes, which do not keep the axial symmetry. In the framework of this model, using the method suggested in Ref. [30], we have obtained an analytical expression for the collective potential as a function of β_{30}. The shape of this potential is completely determined by the experimental data on the parity splitting in the alternating parity band for all considered values of the angular momentum. It is shown below that although for the low values of the angular momentum I the potential energy has a minimum at $\beta_{30} = 0$, nevertheless, at some value of $I = I_{\text{crit}}$ the minimum at $\beta_{30} = 0$

*jolos@theor.jinr.ru

disappears and two minima at nonzero value of β_{30} develop. It is shown below that this is a second order phase transition from reflection-symmetric to reflection-asymmetric shape, which is governed by the angular momentum. The important fact is that we determine the potential for several values of the angular momentum smaller and larger than the critical value of I. This give us the possibility of seeing an evolution of the potential along a sufficiently large interval of the values of the angular momentum, which is the control parameter. Every step of this evolution is determined by data.

The paper is organized in the following way. In Sec. II we determine for all values of the angular momentum the collective potential describing the octupole motion based on the experimental data on parity splitting. In Sec. III, using this potential and applying the Landau theory of phase transitions, we analyze the phase transition phenomena in the alternating parity bands of ^{232}Th, ^{238}U, and ^{240}Pu.

II. DESCRIPTION OF THE MODEL

The Hamiltonian of the model used can be presented as

$$H_I = -\frac{\hbar^2}{2B}\frac{d^2}{d\beta_{30}^2} + V_I(\beta_{30}), \tag{1}$$

where the subscript I indicates that the shape of the potential depends on the angular momentum I. It is assumed here that the quadrupole deformation is rigid. This model has common features with the algebraic model suggested in Ref. [31] and the dinuclear system model [32]. The excitation spectra of these models are characterized by the same set of states (if the number of bosons in Ref. [31] is smaller than their maximum possible number).

In Ref. [30] we did not suggest any parametrizations of V_I but followed the procedure given in the supersymmetric quantum mechanics [33] to obtain a shape of the potential. The experimental data on the parity splitting in the ground state alternating parity bands are used to determine the potential V_I completely. The parity splitting is determined as the difference between the energies of the negative and the positive parity states of the same Hamiltonian. Since in our case the Hamiltonian is given for the fixed value of I, the parity splitting is calculated as a difference between the energies of the negative and the positive parity states for the same I. However, at every value of I in the $K = 0$ band there is only one state with the fixed parity $\pi = (-1)^I$. Thus the energy of the state with the opposite parity but the same I can be introduced only by interpolation using the energies of the states neighboring I and having the parity $(-1)^{I+1}$. For even I the interpolated energy of the unphysical negative parity state is determined using the experimental energies of the negative parity states with the angular momenta $(I-1)$ and $(I+1)$. For odd I the interpolated energy of the unphysical positive parity state is determined using the experimental energies of the positive parity states with the angular momenta $(I-1)$ and $(I+1)$.

We consider making the following ansatz for the positive parity wave function. Since this wave function has no nodes (because it describes the lowest states for every I), we assume that it can be presented by the following expression:

$$\Psi_I(\beta_{30}) = \left(\frac{B\omega}{\pi\hbar}\right)^{\frac{1}{4}} \left\{2\left[1+\exp\left(-\frac{B\omega}{\hbar}\beta_m^2(I)\right)\right]\right\}^{-1/2} \times \left(\exp\left\{-\frac{B\omega}{2\hbar}[\beta_{30}-\beta_m(I)]^2\right\} + \exp\left\{-\frac{B\omega}{2\hbar}[\beta_{30}+\beta_m(I)]^2\right\}\right), \tag{2}$$

which is a sum of two Gaussians centered at $\beta_{30} = \pm\beta_m(I)$ whose width is determined by the parameter ω. Let us rewrite the expression (2) as

$$\Psi_I(\beta_{30}) = \left(\frac{B\omega}{\pi\hbar}\right)^{\frac{1}{4}} \left\{2\left[1+\exp\left(-s_3^2(I)\right)\right]\right\}^{-1/2} \times \left(\exp\left\{-\frac{1}{2}s_3^2(I)[\beta_{30}/\beta_m(I)-1]^2\right\} + \exp\left\{-\frac{1}{2}s_3^2(I)[\beta_{30}/\beta_m(I)+1]^2\right\}\right), \tag{3}$$

where

$$s_3(I) \equiv \sqrt{\frac{B\omega}{\hbar}}\beta_m(I). \tag{4}$$

We see from Eq. (3) that Ψ_I is a function of the variable $[\beta_{30}/\beta_m(I)]$ and depends only on one parameter $s_3(I)$. As shown in the appendix, the potential V_I and the total Hamiltonian H being expressed in terms of the dynamical variable $[\beta_{30}/\beta_m(I)]$ depend on two parameters: a dimensional parameter $\hbar\omega$ and the nondimensional parameter $s_3(I)$. In order to show the wave function Ψ_I and the potential V_I depending on β_{30} we need the value of $\beta_m(I)$, which can be obtained from Eq. (4) if the value of the mass coefficient B is known. To determine B we need experimental data on $B(E1)$. The value of B was determined in this way for ^{240}Pu in Ref. [30], and in Figs. 1–3 the potential and the wave functions are shown depending on the variable β_{30}. We mention that the experimental data on $B(E1)$ are known to have large errors.

Let us clarify the physical meaning of the parameter $s_3(I)$. Since the maximum of the wave function (2) is located at $\beta_{30} = \pm\beta_m$ we can say that β_m is the most probable value of $|\beta_{30}|$. Therefore we can consider this quantity as an effective octupole deformation, although this quantity does not coincide with the position of the minimum of the potential $V_I(\beta_{30})$. The quantity $\sqrt{\hbar/B\omega}$ characterizes the width of the Gaussians in Eq. (3). Thus, $s_3(I)$ is a ratio of the effective octupole deformation in the wave function to the width of a distribution of the octupole deformation. We call $s_3(I)$ an octupole softness parameter. The values of this parameter distinguish well the cases of the rigid octupole deformation and the soft octupole motion. If the width of the Gaussian is going to zero (i.e., the wave function has very narrow maxima at $\beta_{30} = \pm\beta_m$), $s_3(I) \to \infty$. However, if the width is large compared to β_m, $s_3(I) \to 0$.

Following the procedure of the supersymmetric quantum mechanics, we substitute the wave function (3) into the Schrödinger equation with the Hamiltonian (1) and obtain the

following relation for the potential $V_I(\beta_{30})$:

$$V_I = \frac{\hbar^2}{2B}\frac{d^2\Psi_I}{d\beta_{30}^2}/\Psi_I + E_I^*, \tag{5}$$

which gives us

$$V_I(\beta_{30}) = \frac{\hbar\omega}{2}\left\{-1 + s_3^2(I)\left[1+\beta_{30}^2/\beta_m^2(I)\right] - 2s_3^2(I)\frac{\beta_{30}}{\beta_m(I)}\frac{\exp\left[s_3^2(I)\beta_{30}/\beta_m(I)\right] - \exp\left[-s_3^2(I)\beta_{30}/\beta_m(I)\right]}{\exp\left[s_3^2(I)\beta_{30}/\beta_m(I)\right] + \exp\left[-s_3^2(I)\beta_{30}/\beta_m(I)\right]}\right\} + E_I^*, \tag{6}$$

where for even I the quantity E_I^* is the experimental excitation energy of the lowest state with angular momentum I. For odd I this energy is determined by interpolation using the energies of the neighboring even-I states. We assume that $E^*(I)$ and its derivative are the continuous functions of I. As in the case of the wave function the shape of the potential (6) is determined completely by one parameter, namely, $s_3(I)$ only. In Ref. [30] it was shown, based on the results of calculations of the parity splitting $\Delta E(I)$, that the quantity (4) can be parameterized by a linear function of the angular momentum

$$s_3(I) = c_0 + c_1 \cdot I, \tag{7}$$

where c_0 and c_1 are the fit parameters. They are determined so as to get the better description of the angular momentum dependence of the parity splitting $\Delta E(I)$. The values of these parameters, the experimental and the calculated values of the parity splitting $\Delta E(I)$ for ^{232}Th, ^{238}U, and ^{240}Pu, are presented in Tables I–III. As described above, the experimental values of the parity splitting $\Delta E(I)$ are determined using the experimental energies $E_{\rm exp}(I)$ of the positive and the negative parity states of the ground state alternating parity band. We determine the parity splitting as

$$\tfrac{1}{2}\Delta E(I) = \tfrac{1}{2}(-1)^I[E_{\rm inter}(I) - E_{\rm exp}(I)], \tag{8}$$

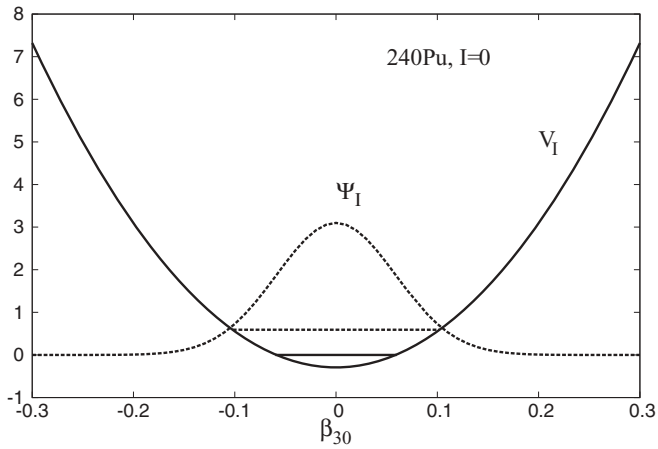

FIG. 1. The potential V_I as a function of β_{30} and the yrast state wave function calculated for $I = 0$ with the parameters fixed for ^{240}Pu. The potential energy is counted from the ground state energy [see Eq. (5)]. The horizontal lines inside the potential well indicate the energies of the lowest (solid line) and the first excited (dashed line) states in this potential. The parity splitting is equal to the difference of the energies of these states.

and the average energy as

$$E_{\rm av}(I) = \tfrac{1}{2}[E_{\rm inter}(I) + E_{\rm exp}(I)], \tag{9}$$

where $E_{\rm inter}(I)$ is the interpolated energy. The details of interpolation used here are described in Refs. [30,34]. The alternative interpolation, which uses the staggering index, has been suggested in Ref. [24].

To obtain the numerical values of β_m we need the value of the mass coefficient B. This mass coefficient is known for ^{240}Pu [30], where we have found from a consideration of $B(E1)/B(E2)$ that $\hbar^2/B$ is approximately equal to $1/496$ MeV. Taking this value and the value of $\hbar\omega$ for ^{240}Pu, we obtain that approximately $s_3(I) = \sqrt{3}\beta_m(I)$. There is no experimental data on the $B(E1)/B(E2)$ ratio between the states of the ground state alternating parity band in ^{232}Th, and in the case of ^{238}U there is experimental information only on decay of the 7_1^- state, which is insufficient to get information about the angular momentum dependence of $B(E1)$. For this reason we cannot determine the mass coefficient B for these nuclei. However, the knowledge of B is not needed to determine the shape of the potential and the critical value of the angular momentum. The last quantity is determined by Eq. (21). Without knowledge of B we obtain the potential as a function of $\beta_{30}/\beta_m(I)$ but not as a function of β_{30}. Thus the scale of β_{30} used to present the potential depends on the angular momentum. However, the value of $I_{\rm crit}$ for which the

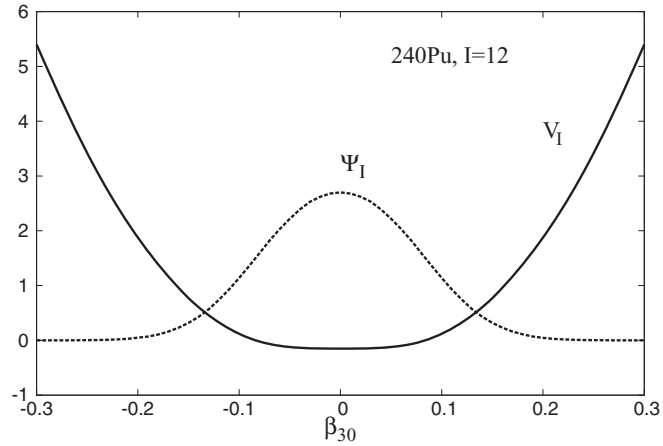

FIG. 2. The potential V_I as a function of β_{30} and the yrast state wave function calculated for $I = 12$ with the parameters fixed for ^{240}Pu. The potential energy is counted from the excitation energy of the 12_1^+ state of ^{240}Pu.

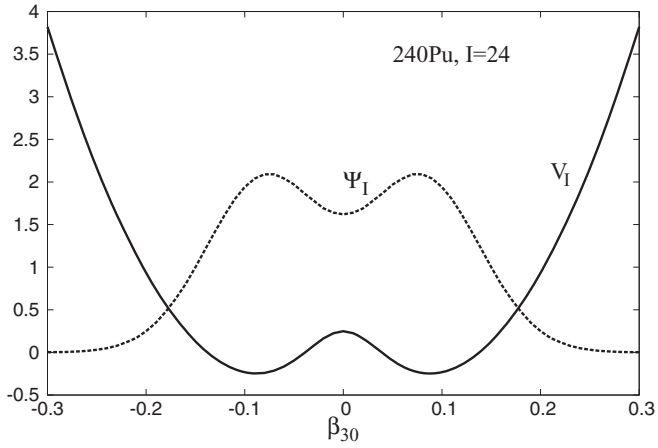

FIG. 3. The potential V_I as a function of β_{30} and the yrast state wave function calculated for $I = 24$ with the parameters fixed for ^{240}Pu. The potential energy is counted from the excitation energy of the 24_1^+ state of ^{240}Pu.

minimum of the potential at $\beta_{30} = 0$ disappears is determined without knowledge of B.

The results for ^{240}Pu are given for completeness in Table III. They have been presented in Ref. [30]. However, we show them here since ^{240}Pu is a nucleus which is investigated better than others. The calculations of $\Delta E(I)$ are performed using the mathematical technique of the supersymmetric quantum mechanics, as was done in Ref. [30].

$\Delta E(I)$ is given by the expression

$$\Delta E(I) = \hbar\omega f[s_3(I)], \tag{10}$$

where the function $f(s_3)$ is determined numerically.

The fact that the experimental data on the parity splitting indicate mainly a linear dependence of $s_3(I)$ on the angular momentum can be explained qualitatively in the following way. The quantity $s_3(I)$ in any case is an increasing function of I. As seen from Eqs. (6) and (4), the potential V_I increases with angular momentum not faster than s_3^2. Indeed, for small s_3 we have

$$V_I(\beta_{30}) = \frac{\hbar\omega}{2}\left(-1 + s_3^2(I) + \frac{B\omega}{\hbar}\beta_{30}^2 - 2s_3^2(I)\frac{B\omega}{\hbar}\beta_{30}^2\right). \tag{11}$$

For large s_3 we can approximate Eq. (6) by the following expression:

$$V_I(\beta_{30}) = \frac{\hbar\omega}{2}\left(-1 + s_3^2(I) + \frac{B\omega}{\hbar}\beta_{30}^2 - 2s_3(I)\sqrt{\frac{B\omega}{\hbar}}|\beta_{30}|\right). \tag{12}$$

Since the potential energy increases with angular momentum approximately proportionally to $I(I+1)$, it is natural to expect a linear dependence of $s_3(I)$ on I.

As seen from the results presented in Tables I–III, they are in a good agreement with the experimental data up to sufficiently high values of the angular momentum I. However, at very high values of I a disagreement is clearly seen between the experimental results and the calculated values. In the cases of ^{232}Th and ^{240} Pu at highest observed values of the angular momentum, the experimental values of $\Delta E(I)$ are lower than the calculated values. However, in the case of ^{238}U, the experimental values of $\Delta E(I)$ at higher values of I are larger than calculated values. An explanation of this phenomena has been suggested in Ref. [39]. At low I the parity splitting shifts the positive parity states down. This is due either to the absence of the barrier at $\beta_{30} = 0$ or to the large probability of a penetration of the barrier that separates two physically equivalent, symmetrically located minima in the nuclear collective potential, depending on the reflection-asymmetric deformation. With an increase in I, the height of the barrier increases also and the barrier penetration probability decreases. Thus, the parity splitting is going to zero. However, at sufficiently high values of I the Coriolis interaction becomes important, producing an alignment in the angular momentum of the intrinsic excitation along the axis of the collective rotation [40–46]. Because of this alignment the same value of the total angular momentum can be obtained with the smaller value of the collective rotational momentum. A decrease of the collective rotational momentum leads to a decrease of the barrier height. Then the barrier penetration probability increases, thus recreating a parity splitting. If the aligned single-particle configuration has an even average parity

TABLE I. The calculated and the experimental values of $\Delta E(I)$ for ^{232}Th. The experimental data are taken from Refs. [35,36]. The following values of the parameters are used: $\hbar\omega = 0.717$ MeV, $c_0 = 0.122$, and $c_1 = 0.040$.

	^{232}Th $\Delta E(I)$ (keV)	
I	Exp	Cal
1	698	698
2	689	688
3	676	676
4	661	662
5	643	646
6	624	629
7	604	610
8	584	590
9	563	569
10	543	547
11	521	525
12	501	502
13	479	478
14	458	455
15	435	432
16	412	408
17	388	385
18	364	363
19	339	342
20	315	320
21	289	299
22	263	279
23	237	260
24	210	242
25	184	224

TABLE II. The calculated and the experimental values of $\Delta E(I)$ for ^{238}U. The experimental data are taken from Ref. [37]. The following values of the parameters are used: $\hbar\omega = 0.683$ MeV, $c_0 = 0.12$, and $c_1 = 0.0462$.

	^{238}U $\Delta E(I)$ (keV)	
I	Exp	Cal
1	665	664
2	656	653
3	642	639
4	625	622
5	605	604
6	584	584
7	560	562
8	535	539
9	509	514
10	484	489
11	457	463
12	432	438
13	407	412
14	384	386
15	361	361
16	340	337
17	320	313
18	303	290
19	287	268
20	274	247
21	263	227
22	255	208
23	248	190
24	245	174
25	242	159
26	241	145
27	239	132
28	235	121

TABLE III. The calculated and the experimental values of $\Delta E(I)$ for ^{240}Pu. The experimental data are taken from Ref. [38]. The following values of the parameters are used: $\hbar\omega = 0.585$ MeV, $c_0 = 0.04$, and $c_1 = 0.055$.

	^{240}Pu $\Delta E(I)$ (keV)	
I	Exp	Cal
1	583	580
2	575	572
3	563	561
4	548	547
5	531	530
6	511	510
7	488	489
8	465	466
9	440	441
10	415	416
11	388	390
12	363	363
13	337	337
14	311	311
15	286	286
16	262	262
17	238	239
18	216	217
19	194	196
20	173	177
21	152	159
22	134	143
23	115	128
24	98	115
25	81	103
26	66	93
27	51	84
28	38	76
29	22	70
30	8	65

then the parity splitting does not change the sign. However, an interval of the values of I for which $\Delta E(I)$ is not equal to zero becomes larger. If the aligned single-particle configuration has an odd average parity then for even values of I the collective wave function should be odd with respect to the transformation $\beta_{30} \to -\beta_{30}$ and vice verse in order to have the total parity of the state equal to $(-1)^I$. As a result, the negative parity states will be shifted down by the parity splitting, in contrast to the situation at low I. However, this effect is not treated in this paper.

Thus, based on the experimental data on the parity splitting, we have determined the parameters c_0 and c_1 for several nuclei. Therefore, we have completely determined the potential for these nuclei at all observed values of the angular momentum. This give us a possibility to investigate the phase transition phenomena in the alternating parity bands of these nuclei.

III. DESCRIPTION OF THE PHASE TRANSITION IN THE ALTERNATING PARITY BANDS

In Figs. 1–3 the octupole potentials determined for ^{240}Pu for three values of the angular momentum, namely, $I = 0$, 12, and 24 are shown. Similar results are obtained for other nuclei. However, we concentrate below on ^{240}Pu, which is investigated experimentally better than other nuclei. The parity splitting given in Tables I–III is equal to the difference between the energies of the first excited and the lowest states in these potentials. It is shown, for example, by two horizontal lines in Fig. 1. Thus the value of E_I^* given in Eq. (5) is unimportant for the calculations of the parity splitting.

It is seen that at $I = 0$ the potential $V_I(\beta_{30})$ has a form of the harmonic oscillator with the minimum at $\beta_{30} = 0$. At $I = 24$ it is a two-minima potential which describes a reflection-asymmetric shape of the nucleus. At $I = 12$ we have a potential corresponding to transition from reflection-symmetric to reflection-asymmetric shape. Although at this value of I a minimum of the potential is located $\beta_{30} = 0$. Thus, with increasing angular momentum the shape phase transition takes place in the alternating parity band.

Let us consider this transition in detail, applying the Landau theory of phase transitions [47,48]. In our case the role of the free energy in the Landau theory is played by the potential V_I

taken at the minimum, β_{30} is an order parameter, and I is a control parameter. We do not use a Taylor expansion of the potential V_I in the order parameter β_{30} since we have an exact analytical expression for this function given by Eq. (6). The next step is the determination of the equilibrium value of the order parameter β_{30}, which is the position of the minimum of the potential. This value of $(\beta_{30})_{\min}$ is a function of the control parameter I. Then we investigate a behavior of the potential and its derivatives at the minimum of the potential.

The position of the minimum of the potential $V_I(\beta_{30})$, that is, the equilibrium value of the order parameter β_{30}, is determined by the condition

$$0 = \left.\frac{dV_I(\beta_{30})}{d\beta_{30}}\right|_{\beta_{30}=(\beta_{30})_{\min}} = \hbar\omega \cdot s_3^2(I)\frac{(\beta_{30})_{\min}}{\beta_m(I)^2} \times \left(1 - \frac{(\beta_{30})_{\min}}{\beta_m(I)}\tanh\left[s_3^2(I)(\beta_{30})_{\min}/\beta_m(I)\right] - \frac{s_3^2(I)}{\left\{\cosh\left[s_3^2(I)(\beta_{30})_{\min}/\beta_m(I)\right]\right\}^2}\right). \quad (13)$$

Let us consider a solution of Eq. (13). This equation is a product of the two terms, namely, $(\beta_{30})_{\min}$ and the expression in parentheses. Because of this the equation has two solutions. The first one is $(\beta_{30})_{\min} = 0$. The second one is given by the root of the following equation:

$$\left(1 - \frac{(\beta_{30})_{\min}}{\beta_m(I)}\tanh\left[s_3^2(I)(\beta_{30})_{\min}/\beta_m(I)\right] - \frac{s_3^2(I)}{\left\{\cosh\left[s_3^2(I)(\beta_{30})_{\min}/\beta_m(I)\right]\right\}^2}\right) = 0. \quad (14)$$

The minimum of V_I at $\beta_{30} = 0$ takes place only if $s_3(I) < \frac{1}{\sqrt{2}}$ when the second derivative of $V_I(\beta_{30})$ over β_{30} at $\beta_{30} = 0$ is positive. If $s_3(I) > \frac{1}{\sqrt{2}}$ then at $\beta_{30} = 0$ potential has a maximum and the minimum is smoothly shifted to nonzero value of β_{30}. This value is determined by the numerical solution of Eq. (14).

If $s_3(I)$ is larger but very close to $\frac{1}{\sqrt{2}}$ the root of Eq. (14) is given approximately as

$$(\beta_{30})_{\min} = \beta_m(I)\sqrt{\frac{3}{2s_3^6(I)}\left(s_3^2(I) - \frac{1}{2}\right)}. \quad (15)$$

Let us find the value of the potential V_I at the minimum. If $s_3(I) < \frac{1}{\sqrt{2}}$ the minimum of the potential is located at $\beta_{30} = 0$ and it follows from Eq. (6) that

$$V_I[(\beta_{30})_{\min}] \equiv V_I(\min) = \frac{1}{2}\hbar\omega\left(-1 + s_3^2(I)\right) + E_I^*, \; s_3(I) < \frac{1}{\sqrt{2}}. \quad (16)$$

For $s_3(I) > \frac{1}{\sqrt{2}}$ but close to $\frac{1}{\sqrt{2}}$

$$V_I(\min) \approx \frac{1}{2}\hbar\omega\left\{-1 + s_3^2(I) - \frac{3}{s_3^4(I)}\left[s_3^2(I) - \frac{1}{2}\right]^2\right\} + E_I^*, \quad s_3(I) > \frac{1}{\sqrt{2}}. \quad (17)$$

In Eq. (17) the terms of the higher order in $[s_3^2(I) - \frac{1}{2}]^2$ are omitted. Remember that according to Eq. (7) $s_3(I)$ is a linear function of I. Comparing Eqs. (16) and (17) we see that $V_I(\min)$ is a continuous function of I at $s_3(I)=\frac{1}{\sqrt{2}}$. Taking the first order derivatives of the expressions (16) and (17) we see that both derivatives coincide at $s_3 = \frac{1}{\sqrt{2}}$. However, there is a discontinuity of the second order derivative over I at $s_3(I)=\frac{1}{\sqrt{2}}$. Indeed, for $s_3(I) < \frac{1}{\sqrt{2}}$

$$\frac{d^2V_I(\min)}{dI^2} = \hbar\omega c_1^2 + \frac{d^2E_I^*}{dI^2}, \quad s_3(I) < \frac{1}{\sqrt{2}}. \quad (18)$$

For $s_3(I) > \frac{1}{\sqrt{2}}$

$$\frac{d^2V_I(\min)}{dI^2} = \hbar\omega c_1^2\left\{1 - \frac{12}{s_3^2(I)} + \frac{42}{s_3^4(I)}\left[s_3^2(I) - \frac{1}{2}\right] - \frac{30}{s_3^6(I)}\left[s_3^2(I) - \frac{1}{2}\right]^2 + \cdots\right\} + \frac{d^2E_I^*}{dI^2}, \quad s_3(I) > \frac{1}{\sqrt{2}}. \quad (19)$$

At the critical point $s_3(I) = \frac{1}{\sqrt{2}}$ the expressions (18) and (18) differ by the term $-12\hbar\omega c_1^2/s_3^2(I)$. Thus, we have a second order phase transition. This is a transition from reflection-symmetric to reflection-asymmetric shape in the alternating parity band at the value of the angular momentum.

Let us introducing a special notation for the critical value of s_3, which is equal, as shown above, to $\frac{1}{\sqrt{2}}$

$$s_{3,\mathrm{crit}} = \frac{1}{\sqrt{2}}. \quad (20)$$

The corresponding critical value of the angular momentum I_{crit} is determined according to Eq. (7) by the relation

$$c_0 + c_1 \cdot I_{\mathrm{crit}} = \frac{1}{\sqrt{2}}. \quad (21)$$

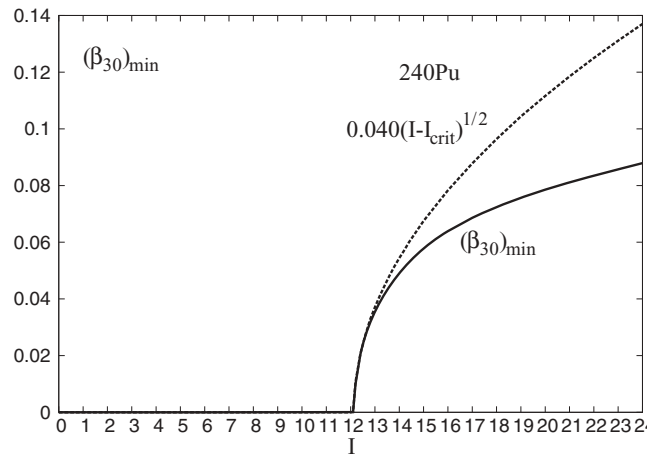

FIG. 4. Exact dependence of $(\beta_{30})_{\min}$ on the angular momentum calculated for ^{240}Pu using Eq. (13) (solid line) and an approximate description of $(\beta_{30})_{\min}$ by a square root function valid around $I = I_{\mathrm{crit}}$ (dashed line) given by Eq. (22).

TABLE IV. The calculated values of the critical angular momentum I_{crit} and the parameters c_0, c_1, and $\hbar\omega$.

Nucleus	I_{crit}	c_0	c_1	$\hbar\omega$ (MeV)
^{232}Th	14.6	0.122	0.0400	0.717
^{238}U	12.7	0.120	0.0462	0.683
^{240}Pu	12.1	0.040	0.055	0.595

Now we can rewrite expression (15) in the following way:

$$(\beta_{30})_{\min} = \beta_m(I_{crit})(12\sqrt{2}c_1(I - I_{crit}))^{1/2}. \quad (22)$$

In this derivation the linear relation between s_3 and I given by Eq. (7) is used. Equation (22) holds in the vicinity of the critical point. We see that the critical exponent is equal to 1/2.

An exact dependence of $(\beta_{30})_{\min}$ on the value of the angular momentum obtained numerically from Eq. (14) is shown in Fig. 4 for ^{240}Pu. An approximate dependence of $(\beta_{30})_{\min}$ described by Eq. (22) is also shown in this figure for comparison. We see that the approximate expression holds in some interval of the values of I above I_{crit}. We see in Fig. 4 that $(\beta_{30})_{\min}$ is equal to zero for all values of the angular momentum below $I = I_{crit}$. However, at $I = I_{crit}$ there is a cusp in the dependence of $(\beta_{30})_{\min}$ on I and $(\beta_{30})_{\min}$ increases smoothly for higher values of I. Similar results are obtained for the other considered nuclei.

As mentioned in connection with the Hamiltonian (1), it is assumed that the quadrupole deformation is rigid. This restricts our consideration to the quadrupole well-deformed nuclei.

Due to the fact that the measurements extend to high values of I, the control parameter, namely the angular momentum, takes several values below and above its critical value. This allows us to explore the critical point and its neighborhood in great detail as shown in Fig. 4.

Thus, $s_{3,crit}$ plays the role of that value of $s_3(I)$ at which appears the reflection-asymmetric deformation. Remember that the parameters c_0 and c_1 are determined for all considered nuclei by the experimental data on parity splitting $\Delta E(I)$.

The values of I_{crit} determined for ^{232}Th, ^{238}U, and ^{240}Pu are shown in Table IV. We put also in this table the values of the parameters c_0, c_1, and $\hbar\omega$ in order to see their evolution with nucleus.

Since our analysis of the phase transition is semiclassical, it is not strange that the relation (21) gives noninteger values for I_{crit}. Coming back to Tables I–III, we see that for all considered nuclei there are at least five values of I larger than I_{crit} for which we have a good description of the parity splitting. Parity splitting is also well described for I smaller than I_{crit}. So, we can see an evolution of the potential from the reflection-symmetric to the reflection-asymmetric cases going through the phase transition point along a sufficiently large interval of the values of the angular momentum.

IV. SUMMARY

In summary, we have shown that the experimental data on the spectra of the ground state alternating parity bands of several actinides indicate a second order phase transition from reflection-symmetric to reflection-asymmetric shapes in these bands. The phase transition takes place at some value of the angular momentum, which in our consideration plays the role of the control parameter. Our approach is based on the assumption that the main role in the description of the properties of the alternating parity bands is played by the octupole mode, preserving the axial symmetry. It is shown that this approach provides a good description of the experimental data on parity splitting for all values below and several values above the critical value of I. So, we have a possibility to see an evolution of the potential depending on the order parameter β_{30} at the sufficiently large interval of the values of the angular momentum. This allows us to explore the critical point and its neighborhood in great detail.

ACKNOWLEDGMENTS

The authors are grateful to Profs. A. Gelberg, W. Scheid, and I. Wiedenhöver for useful discussions. One of us (R.V.J.) thanks colleagues from the University of Cologne for their kind hospitality. This work was supported by the DFG (Germany) under Contract Br 799/25-1, by RFBR under Grant No. 10-02-00301, and by the Heisenberg-Landau Program.

APPENDIX

In this appendix we present the expression for the total Hamiltonian expressed in terms of the dynamical variable $\beta_{30}/\beta_m(I)$:

$$H_I = \frac{1}{2}\hbar\omega\Bigg(- \frac{1}{s_3^2(I)}\frac{d^2}{d[\beta_{30}/\beta_m(I)]^2} + \frac{1}{s_3^2(I)}\frac{d^2\Psi_I[s_3(I), \beta_{30}/\beta_m(I)]}{d[\beta_{30}/\beta_m(I)]^2} \times \frac{1}{\Psi_I[s_3(I), \beta_{30}/\beta_m(I)]}\Bigg) + E_I^*. \quad (A1)$$

[1] A. E. L. Dieperink, O. Scholten, and F. Iachello, Phys. Rev. Lett. **44**, 1747 (1980).
[2] A. E. L. Dieperink and O. Scholten, Nucl. Phys. A **346**, 125 (1980).
[3] J. Jolie, R. F. Casten, P. von Brentano, and V. Werner, Phys. Rev. Lett. **87**, 162501 (2001).
[4] J. Jolie, P. Cejnar, R. F. Casten, S. Heinze, A. Linnemann, and V. Werner, Phys. Rev. Lett. **89**, 182502 (2002).
[5] F. Iachello and N. V. Zamfir, Phys. Rev. Lett. **92**, 212501 (2004).
[6] A. Frank, P. Van Isacker, and F. Iachello, Phys. Rev. C **73**, 061302(R) (2006).
[7] R. F. Casten, Nat. Phys. **2**, 811 (2006).

[8] P. Cejnar, J. Jolie, and R. F. Casten, Rev. Mod. Phys. **82**, 2155 (2010).
[9] J. Kotila, K. Nomura, L. Guo, N. Shimizu, and T. Otsuka, Phys. Rev. C **85**, 054309 (2012).
[10] A. Dewald, O. Möller, B. Saha *et al.*, J. Phys. G **31**, s1427 (2005).
[11] A. Dewald, O. Möller, D. Tonev *et al.*, Eur. Phys. J. A **20**, 173 (2004).
[12] F. Iachello, Phys. Rev. Lett. **85**, 3580 (2000).
[13] F. Iachello, Phys. Rev. Lett. **87**, 052502 (2001).
[14] P. G. Bizzeti and A. M. Bizzeti-Sona, Phys. Rev. C **70**, 064319 (2004).
[15] P. G. Bizzeti and A. M. Bizzeti-Sona, Eur. Phys. J. A **20**, 179 (2004).
[16] P. G. Bizzeti and A. M. Bizzeti-Sona, Phys. Rev. C **77**, 024320 (2008).
[17] D. Bonatsos, D. Lenis, N. Minkov, D. Petrellis, and P. Yotov, Phys. Rev. C **71**, 064309 (2005).
[18] P. Cejnar and J. Jolie, Phys. Rev. C **69**, 011301(R) (2004).
[19] P. Cejnar, M. Macek, S. Heinze, J. Jolie, and J. Dobeš, J. Phys. A: Math. Gen. **39**, L515 (2006).
[20] M. A. Caprio, P. Cejnar, and F. Iachello, Ann. Phys. (NY) **323**, 1106 (2008).
[21] A. Bohr and B. Mottelson, *Nuclear Structure* (Benjamin, New York, 1975), Vol. 2.
[22] H. J. Wollersheim, H. Emling, H. Grein *et al.*, Nucl. Phys. A **556**, 261 (1993).
[23] W. Nazarewicz and S. L. Tabor, Phys. Rev. C **45**, 2226 (1992).
[24] I. Ahmad and P. A. Butler, Ann. Rev. Nucl. Part. Sci. **43**, 71 (1993).
[25] P. Butler and W. Nazarewicz, Rev. Mod. Phys. **68**, 349 (1996).
[26] J. F. C. Cocks, P. A. Butler, K. J. Cann *et al.*, Phys. Rev. Lett. **78**, 2920 (1997).
[27] I. Wiedenhöver, R. V. F. Janssens, G. Hackman *et al.*, Phys. Rev. Lett. **83**, 2143 (1999).
[28] R. F. Casten and N. V. Zamfir, Phys. Rev. Lett. **85**, 3584 (2000).
[29] R. M. Clark, M. Cromaz, M. A. Deleplanque *et al.*, Phys. Rev. C **69**, 064322 (2004).
[30] R. V. Jolos and P. von Brentano, Phys. Rev. C **84**, 024312 (2011).
[31] F. Iachello and A. D. Jackson, Phys. Lett. B **108**, 151 (1982).
[32] T. M. Shneidman, G. G. Adamian, N. V. Antonenko, R. V. Jolos, and W. Scheid, Phys. Lett. B **526**, 322 (2002).
[33] F. Cooper, A. Khare, and U. Sukhatme, *Supersymmetry in Quantum Mechanics* (World Scientific, Singapore, 2004).
[34] R. V. Jolos and P. von Brentano, Nucl. Phys. A **587**, 377 (1995).
[35] R. S. Simon, R. P. Devito, H. Emling *et al.*, Phys. Lett. B **108**, 87 (1982).
[36] P. C. Sood, D. M. Headly, and R. K. Sheline, At. Data Tables **47**, 89 (1991); **51**, 273 (1992).
[37] D. Ward, H. A. Andrews, C. C. Ball *et al.*, Nucl. Phys. A **600**, 88 (1996).
[38] X. Wang, R. V. F. Janssens, M. P. Carpenter *et al.*, Phys. Rev. Lett. **102**, 122501 (2009).
[39] R. V. Jolos, N. Minkov, and W. Scheid, Phys. Rev. C **72**, 064312 (2005).
[40] K. Neergard and P. Vogel, Nucl. Phys. A **145**, 33 (1970).
[41] K. Neergard and P. Vogel, Nucl. Phys. A **149**, 217 (1970).
[42] P. Vogel, Phys. Lett. B **60**, 431 (1976).
[43] Ch. Briancon and I. N. Mikhailov, Sov. J. Part. Nucl. **13**, 101 (1982).
[44] I. N. Mikhailov, R. K. Safarov, F. N. Usmanov, and Ch. Briancon, Yad. Fis. **38**, 297 (1983).
[45] R. G. Nazmitdinov, I. N. Mikhailov, and Ch. Briancon, Phys. Lett. B **188**, 171 (1987).
[46] S. Frauendorf, Phys. Rev. C **77**, 021304(R) (2008).
[47] L. Landau, Phys. Z. Sowjetunion **11**, 26 (1937).
[48] L. D. Landau and E. M. Lifshitz, *Statistical Physics*, Course of Theoretical Physics, Part 1, Vol. V (Butterworth-Heinemann, Oxford, 2001).